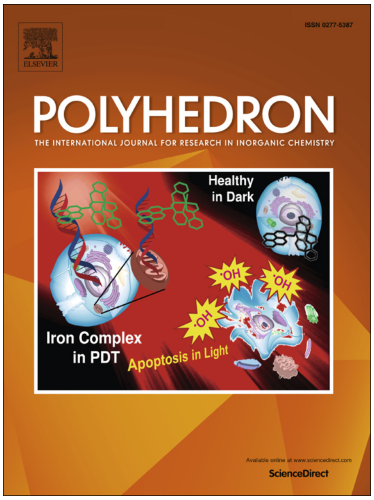

A rhodium(I) dicarbonyl complex with a redox-active ferrocenyl phosphine-NHC ligand: enhanced reactivity of the metal centre through ferrocene oxidation

Nathalie Debono, Jean-Claude Daran, Rinaldo Poli, Agnès Labande

PII: S0277-5387(14)00270-8
DOI: http://dx.doi.org/10.1016/j.poly.2014.04.050
Reference: POLY 10694

To appear in: *Polyhedron*

Received Date: 21 February 2014
Accepted Date: 26 April 2014

Please cite this article as: N. Debono, J-C. Daran, R. Poli, A. Labande, A rhodium(I) dicarbonyl complex with a redox-active ferrocenyl phosphine-NHC ligand: enhanced reactivity of the metal centre through ferrocene oxidation, *Polyhedron* (2014), doi: http://dx.doi.org/10.1016/j.poly.2014.04.050

A rhodium(I) dicarbonyl complex with a redox-active ferrocenyl phosphine-NHC ligand: enhanced reactivity of the metal centre through ferrocene oxidation

Nathalie Debono,[a,b] Jean-Claude Daran,[a,b] Rinaldo Poli [a,b,c] and Agnès Labande*[,a,b]

a. CNRS, LCC (Laboratoire de Chimie de Coordination), 205 route de Narbonne, BP 44099, F-31077 Toulouse Cedex 4, France. E-mail: agnes.labande@lcc-toulouse.fr; Fax: (+33) 561553003; Tel: (+33) 561333158
b. Université de Toulouse, UPS, INPT, F-31077 Toulouse Cedex 4, France
c. Institut Universitaire de France, 103 bd Saint-Michel, F-75005 Paris, France

This paper is dedicated to Professor Claude Lapinte on the occasion of his retirement.

Abstract

A rhodium(I) dicarbonyl complex bearing a bidentate ferrocenyl phosphine-NHC ligand has been synthesized and characterized by NMR, IR spectroscopy, mass spectrometry and X-Ray diffraction methods. Its behaviour towards oxidation was investigated and revealed that changing the oxidation state of ferrocene can significantly modify the electron density at rhodium. Oxidation of the rhodium(I) dicarbonyl complex in acetonitrile furnished an air-stable rhodium(III) complex, stabilized by acetonitrile molecules and with an interesting C-H bond activation at ferrocene. This new rhodium(III) complex is active for the hydrosilylation of acetophenone and its derivatives.

1. Introduction

Wrighton et al. first demonstrated in the early 1990s that fine tuning of the electronic properties of a metal complex could be achieved by the introduction of redox-active ligands, as they were able to enhance the reactivity of a carbonyl ligand coordinated to rhenium towards nucleophiles by changing the oxidation state of cobaltocene [1]. In the area of catalysis, Mirkin also described the use of hemilabile redox-active ligands that presented charge-dependent behaviour [2]. Later, Gibson and Long showed that they could reversibly modulate the activity of a titanium polymerisation catalyst with the help of a substitutionally inert, redox-active ligand [3]. More recent examples include the work of Bielawski [4-6], Diaconescu [7,8] and Plenio [9,10].

Many redox-active groups have been incorporated, such as the ubiquitous ferrocene [2-5,9-13], or other metallocenes [1,14], quinone [6], terthienyl [15], amidophenolates [16], etc. However, it was only recently that the redox properties of N-heterocyclic carbenes (NHC) bearing electroactive groups were exploited in catalysis. The NHC can either be in direct electronic communication with the electroactive moiety (ferrocene [5], quinone [6]), or simply act as an ancillary ligand or "anchor" to guarantee the stability of the complex whatever the oxidation state of the electroactive component [9].

Our group has a strong interest in the chemistry and catalytic activity of functionalised N-heterocyclic carbene complexes [17-21]. We have recently investigated the behaviour of a 1,5-cyclooctadiene (COD) rhodium(I) complex bearing a ferrocenyl phosphine-NHC ligand, **1**, towards oxidation (figure 1) [21]. We have been able to demonstrate that iron oxidation has dramatic consequences on the reactivity of the rhodium complex, and we then wished to extend this work to a similar rhodium(I) complex possessing carbonyl ligands in place of COD. The results of these studies are described here.

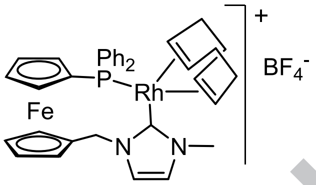

1

Figure 1. Rhodium(I) complex **1** with redox-active ferrocenyl phosphine-NHC ligand.

2. Experimental

General considerations

All manipulations were carried out under an inert atmosphere of dry argon by using vacuum line and Schlenk tube techniques. Solvents for all syntheses were dried and degassed by standard methods before use, unless otherwise stated.

The 1D- and 2D-NMR spectra were recorded on Bruker AV500 and AV400 spectrometers. ^{1}H and ^{13}C chemicals shifts (δ) are given in ppm (the residual peak of deuterated solvents was used as reference). ^{31}P chemicals shifts are reported in ppm. Peaks are labelled as singlet (s), doublet (d), triplet (t), multiplet (m) and broad (br). The proton and carbon assignment were performed by COSY, HSQC, ^{1}H-^{13}C HMBC, ^{1}H-^{31}P HMBC experiments. The IR spectra were acquired on a Bruker Alpha-P spectrometer equipped with an ATR module (compound **2**) or Perkin-Elmer Spectrum 100 FT-IR with an ATR module (compound **3**). The MS spectra were obtained from the mass spectrometry service of the Paul Sabatier University. The cyclic voltammetry (CV) experiment was carried out with a PGSTAT-302N potentiostat (Metrohm) at 25°C using a Pt disk working electrode, a Pt wire counter electrode and a saturated calomel reference electrode (SCE); a 0.1 M n-Bu_4BF_4 solution was used as the supporting electrolyte. The solution used during the electrochemical study was typically 10^{-3} M in rhodium compound. All electrochemical data are referenced versus ferrocene (in our hands, E°[FcH/FcH^{+}] = 0.54 V/SCE in CH_2Cl_2/n-Bu_4BF_4, 0.1 V.s^{-1}, 25°C).

The rhodium(I) complex **1** [17] and thianthrenium tetrafluoroborate $[Th][BF_4]$ [22] were prepared according to previously reported procedures.

Abbreviations

Cp^P: cyclopentadienyl ring with the PPh_2 substituent.

Cp^C: cyclopentadienyl ring with the NHC substituent.

Fc: ferrocenyl.

Im: imidazol-2-ylidene.

L: ferrocenyl phosphine-NHC ligand.

Syntheses

$[Rh(CO)_2(L)]^+BF_4^-$ (**2**)

CO was bubbled through a solution of complex **1** (50 mg, $7.0 \cdot 10^{-5}$ mole) in CH_2Cl_2 (30 mL) for 2h. After partial solvent evaporation, a yellow solid was obtained by precipitation with pentane. The solution was filtered off and the solid was washed twice with pentane to remove the 1,5-cyclooctadiene, then dried in vacuo. The solid was obtained as a yellow powder (42 mg, 91%). IR (ATR): 2085 (s), 2029 (s) cm^{-1} ($\nu_{C=O}$). Occasionally, isolated samples of the product obtained from incomplete carbonylations gave a spectrum featuring a third $\nu_{C=O}$ vibration at 1997 (m) cm^{-1}, assigned to the monocarbonyl complex (≤5%); ^1H NMR (400.13 MHz, $CDCl_3$, 298 K): δ 7.71 (1H, d, J_{HH}= 2.0 Hz, *H*C=C Im), 7.63-7.53 (6H, m, PPh_2), 7.50-7.45 (2H, m, PPh_2), 7.43 (1H, d, J_{HH}= 2.0 Hz, *H*C=C Im), 7.35-7.28 (2H, m, PPh_2), 5.17 (1H, d, J_{HH}= 14.8 Hz, CH_2 Im), 4.89 (1H, d, J_{HH}= 15.2 Hz, CH_2 Im), 4.70 (1H, m, Cp^C), 4.61 (1H, m, Cp^P), 4.57 (1H, m, Cp^C), 4.40 (1H, m, Cp^P), 4.28 (1H, m, Cp^C), 4.18 (1H, m, Cp^C), 3.47 (1H, br s, Cp^P), 3.25 (3H, s, CH_3), 2.51 (1H, br s, Cp^P). ^{13}C NMR (100.62 MHz, $CDCl_3$, 298 K): δ 186.7 (dd, J_{RhC}= 55.7 Hz, J_{PC}= 16 Hz, *C*O), 181.8 (dd, J_{RhC}= 61.2 Hz, J_{PC}= 102.3 Hz, *C*O), 165.9 (dd, J_{RhC}= 16.2 Hz, J_{PC}= 42.1 Hz, $C_{carbene}$), 133.4 (d, J_{PC}= 12.5 Hz, CH_{PPh2}), 132.7 (d, J_{PC}= 12.4 Hz, CH_{PPh2}), 132.5 (quat C_{PPh2}), 131.9 (dd, J_{RhC}= 2.0 Hz, J_{PC}= 10.0 Hz, CH_{PPh2}), 131.1 (d, J_{PC}= 46.7 Hz, quat C_{PPh2}), 129.6 (d, J_{PC}= 10.5 Hz, CH_{PPh2}), 129.0 (d, J_{PC}= 10.8 Hz, CH_{PPh2}), 125.6 (2*C=C Im), 88.0 (quat Cp^C), 75.1 (d, J_{PC}= 7.7 Hz, Cp^P), 74.4 (Cp^C), 73.3 (d, J_{PC}= 7.5 Hz, Cp^P), 72.8 (d, J_{PC}= 14.4 Hz, Cp^P), 72.0 (d, J_{PC}= 6.6 Hz, Cp^P), 70.1 (Cp^C), 69.5 (Cp^C), 68.7 (Cp^C), 68.4 (d, J_{PC}= 60.1 Hz, quat Cp^P), 49.0 (CH_2 Im), 37.6 (CH_3 Im). ^{31}P NMR (161.98 MHz, $CDCl_3$, 298 K): δ 19.98 (d, J_{RhP}= 132 Hz). MS (ESI): m/z 595 [M-CO] (11), 384 $[M-C_6H_4N_2O_2Rh]$ (96). HRMS (ES^+): calcd for $C_{29}H_{25}FeN_2O_2PRh$ 623.0058; found 623.0061.

Oxidation of $[Rh(CO)_2(L)]^+BF_4^-$ (**2**) in CH_2Cl_2

In a glovebox, $AgBF_4$ (10 mg, 0.049 mmol, 1.5 equiv.) was added, as a solid, to a solution of complex **2** (23 mg, 0.033 mmol) in CH_2Cl_2 (3 mL). The solution turned from yellow to deep green in a few seconds. Stirring was stopped to allow the silver precipitate to settle and an aliquot of the solution was deposited on the IR cell. After evaporation of the solvent, the green solid was analysed: IR (ATR) 2097 (s), 2045 (s) cm^{-1} ($\nu_{C=O}$).

Oxidation of $[Rh(CO)_2(L)]^+BF_4^-$ (**2**) in MeCN: generation of $[Rh(CH_3CN)_3(L)](BF_4)_2$ (**3**)

A solution of thianthrenium tetrafluoroborate (27 mg, $8.9{\cdot}10^{-5}$ mole, 1.5 equiv.) in CH_3CN (2.5 mL) was added dropwise to a solution of **2** (42 mg, $5.9{\cdot}10^{-5}$ mole, 1 equiv.) in CH_3CN (5 mL). The mixture was stirred for 10 min at room temperature and then the solvent was evaporated in vacuo. The complex was precipitated with a CH_3CN/Et_2O (1/9) mixture several times until the solution was colourless, then taken up into CH_3CN and left standing for 48h. The solvent was evaporated in vacuo to give **3** as an orange solid (38.8 mg, 76%). IR (ATR) ν_{max}/cm^{-1} 2322, 2293 and 2252 (w) ($C{\equiv}N_{str.}$); 1474, 1436 and 1405 (w/m) ($C{=}C_{str.}$); 1051-999 (vs) (BF_4); 747, 696 and 684 (m/s) ($C\text{-}H_{bend.}$). ^{1}H NMR (500.33 MHz, CD_3CN, 228 K): δ 7.65-7.55 (3H, m, PPh_2), 7.53-7.46 (4H, m, *H*C=C Im + PPh_2), 7.43-7.40 (2H, m, PPh_2), 7.20 (1H, s, *H*C=C Im), 7.11 (2H, dd, J_{HH}= 11.5 Hz, J_{HP}= 7.5 Hz, PPh_2), 5.63 (1H, br s, Cp^P), 4.89 (1H, d, J_{HH}= 16.1 Hz, CH_2 Im), 4.73-4.66 (4H, m, Cp^C + 2 x Cp^P + CH_2 Im), 4.58 (1H, s, Cp^C), 4.40 (1H, s, Cp^P), 4.18 (1H, s, Cp^C), 3.98 (3H, s, CH_3). ^{13}C NMR (125.82 MHz, CD_3CN, 228 K): δ 147.2 (dd, J_{RhC}= 47.2 Hz, J_{PC}= 11.4 Hz, $C_{carbene}$), 133.1-132.6 (m, 2 x *o*-CH_{PPh2} + *p*-CH_{PPh2}), 132.0 (d, J_{PC}= 9.8 Hz, 2 x *o*-CH_{PPh2}), 131.3 (d, J_{PC}= 2.6 Hz, *p*-CH_{PPh2}), 129.6 (d, J_{PC}= 10.9 Hz, 2 x *m*-CH_{PPh2}), 128.5 (d, J_{PC}= 10.7 Hz, 2 x *m*-CH_{PPh2}), 128.0 (d, J_{PC}= 52.2 Hz, quat C_{PPh2}), 126.3 (C=C Im), 124.1 (C=C Im), 123.9 (quat C), 122.17 (d, quat C), 87.2 (br s, quat Cp^C), 83.3 (d, J_{PC}= 9.1 Hz, Cp^P), 77.1 (d, J_{PC}= 12.6 Hz, Cp^P), 75.3 (Cp^C), 73.7 (d, J_{PC}= 7.2 Hz, Cp^P), 73.3 (d, J_{PC}= 6.9 Hz, Cp^P), 72.3 (Cp^C), 71.4 (d, J_{PC}= 65.8 Hz, quat Cp^P), 70.6 (Cp^C), 50.4 (CH_2 Im), 39.1 (CH_3). ^{31}P NMR (202.54 MHz, CD_3CN, 228 K): δ 41.56 (d, J_{RhP}= 138 Hz).

General procedure for the hydrosilylation of acetophenone derivatives

The rhodium catalyst ($4{\cdot}10^{-6}$ mole, 1 mol%) was placed in a dry Schlenk tube under argon and THF (0.2 mL) and acetophenone ($3.9{\cdot}10^{-4}$ mole, 1 equiv., 2.0 M in THF) were added. Diphenylsilane ($4.3{\cdot}10^{-4}$ mole, 1.1 equiv.) was then added dropwise at room temperature and the resulting mixture was stirred for 17h. The solvent was concentrated in vacuo, the residue taken up into CH_2Cl_2 and MeOH (1 mL) and stirred for 1h. HCl (2 M, 1 mL) was then added and the mixture was stirred for an additional hour. The phases were separated, the aqueous phase extracted with CH_2Cl_2 and the organic phases were dried ($MgSO_4$), filtered and concentrated in vacuo. The residue was analysed by ^{1}H NMR ($CDCl_3$) and the conversions were calculated by integration and comparison of the characteristic signals of acetophenone (δ 2.63, s, 3H) and 1-phenylethanol (δ 4.90, q, 1H).

Kinetic follow-up: the rhodium catalyst ($8{\cdot}10^{-6}$ mole, 1 mol%) was placed in a dry NMR tube under argon and d_8-THF (0.4 mL) and acetophenone ($7.9{\cdot}10^{-4}$ mole, 1 equiv., 2.0 M in THF) were added. Diphenylsilane ($8.7 \cdot 10^{-4}$ mole, 1.1 equiv.) was then added dropwise at room temperature and the resulting mixture was shaken. The reaction mixture was analysed by ^{1}H NMR and the conversions were calculated by integration and comparison of the characteristic signals of acetophenone (δ 2.50, s, 3H) and diphenyl(1-phenylethoxy)silane (δ 1.53, d, 3H).

X-ray structural analyses

A single crystal of compound **2** was mounted under inert perfluoropolyether at the tip of a glass fiber and cooled in the cryostream of an Oxford-Diffraction Xcalibur CCD diffractometer. The structure was solved by direct methods (SIR97 [23]) and refined by least-squares procedures on F^2 using SHELXL-97 [24]. All H atoms attached to carbon were introduced in calculation in idealized positions and treated as riding models. The drawing of the molecules was realized with the help of ORTEP32 [25].

Crystal data for compound **2**: yellow needles, $C_{29}H_{25}FeN_2O_2PRh \cdot BF_4$, M= 710.05, monoclinic, a = 9.5352(3), b = 21.1742(7), c = 13.8059(4) Å, β = 101.32 (3) °, V = 2734.97(15) Å^3, T = 180 K, space group $P2_1/n$ (no 14), Z= 4, μ(Mo-$K\alpha$)= 1.25 mm^{-1}, 29805 reflections measured, 6010 unique (R_{int}= 0.032) which were used in all calculations, 5029 observed with $I \geq 2\sigma(I)$, 389 parameters, 17 restraints. The final R and $wR(F^2)$ were 0.027 and 0.067 respectively(all data), GOF, 0.98.

3. Results and discussion

1. Synthesis and characterisation of the rhodium(I) dicarbonyl complex 2

The synthesis of the precursor rhodium complex **1** was reported in a previous work [17]. It is perfectly air stable and was not altered after several months of storage. Its ^{31}P NMR spectrum shows a doublet at δ 19.5 (J_{Rh-P}= 158 Hz), whereas the ^{13}C NMR spectrum shows a doublet of doublets situated at δ 176.9 ($^{1}J_{Rh-C}$= 49.7 Hz, $^{2}J_{P-C}$= 15.5 Hz), typical of the C2 carbon in Rh(I) NHC complexes.

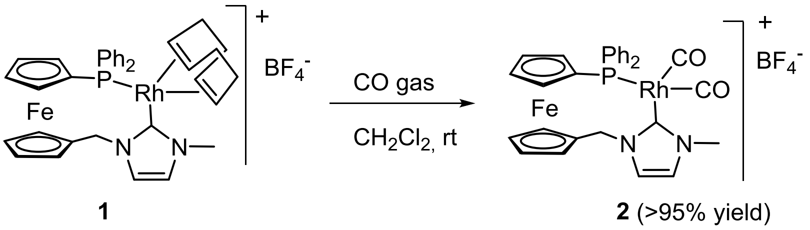

Scheme 1. Synthesis of rhodium(I) carbonyl complex **2**.

The dicarbonyl complex **2** was prepared in quasi-quantitative yield, as verified by ^{31}P NMR monitoring, by bubbling CO gas through a solution of **1** in CH_2Cl_2 (scheme 1). As observed for other cationic Rh(I) complexes [26,27], the resulting pale yellow solid is moderately stable in solution and decomposes in a few days when left in air. It is stable under argon in the solid form, however, and was fully characterised by conventional methods. Its ^{31}P NMR spectrum shows a doublet at δ 20.5, with a smaller coupling constant to rhodium ($J_{Rh\text{-}P}$= 132 Hz) than that of complex **1**. The ^{1}H NMR spectrum revealed the disappearance of the COD proton signals, whereas typical signals for coordinated CO ligands were attributed in the ^{13}C NMR spectrum at δ 186.7 (dd, $^{1}J_{Rh\text{-}C}$= 55.7 Hz, $^{2}J_{P\text{-}C}$= 16.0 Hz, *cis* to P) and 181.8 (dd, $^{1}J_{Rh\text{-}C}$= 61.2 Hz, $^{2}J_{P\text{-}C}$= 102.3 Hz, *trans* to P). The characteristic ^{13}C NMR signal of the C2 carbon (dd, δ 165.9, $^{1}J_{Rh\text{-}C}$= 42.1 Hz, $^{2}J_{P\text{-}C}$= 16.2 Hz) was found upfield compared to that of complex **1**, which is consistent with similar Rh(I) NHC complexes [26,28]. Finally infra-red spectroscopy, which is a very useful tool for the characterisation of carbonyl compounds, showed two intense bands for ν_{CO} stretching frequencies at 2084 and 2029 cm^{-1}, which are in accord with other cationic NHC-Rh complexes [26,27]. The presence of two bands of equal intensity is consistent with the expected *cis* arrangement of the two carbonyl groups.

X-ray quality crystals of **2** were obtained by slow diffusion of pentane into a CH_2Cl_2 solution of the complex under 1 atm of CO, the diffraction analysis of which confirmed the expected structure (fig. 2), with a typical square-planar geometry about the rhodium atom. The structure does not present any unusual features. Selected bond lengths and angles are listed in Table 1. The carbene-rhodium and phosphorus-rhodium bond lengths are consistent with those measured in related Rh(I)-NHC complexes [28,29] and are similar, within errors, to those measured for the previously described Rh(I)-NHC COD complex **1** [17]. The Rh-carbonyl bond lengths are also within the expected range for this type of compounds.

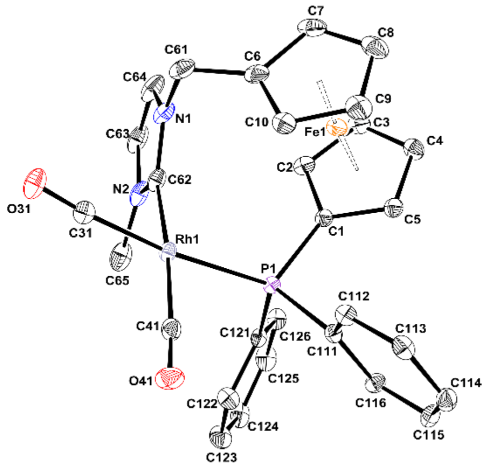

Figure 2. ORTEP representation of the cation in the dicarbonyl complex **2**. Ellipsoids are shown at the 30% probability level. All hydrogen atoms are omitted for clarity.

Table 1. Selected bond distances (Å) and angles (°) for the experimental structure of **2** and comparison with those of **1** [17].

Bond	Complex **1** [17]	Complex **2**
Rh(1)-C(NHC)	2.047(3)	2.062(2)
Rh(1)-P(1)	2.3345(8)	2.3547(6)
Rh(1)-C(L) (**1**, L=(COD); **2**, L=CO)	2.215(3), 2.231(3) 2.220(3), 2.217(3)	1.901(3) 1.886(3)
O(31)-C(31)	-	1.124(3)
O(41)-C(41)	-	1.128(3)
Angle		
C(NHC)-Rh(1)-P(1)	90.83(8)	89.92(7)
C(41)-Rh(1)-P(1)	-	91.93(7)
C(31)-Rh(1)-C(62)	-	86.78(10)
C(31)-Rh(1)-C(41)	-	91.97(10)

2. Oxidation studies

The rhodium complex **2** was analysed by electrochemical methods. The cyclic voltammogram of **2** was recorded in CH_2Cl_2 (fig. 3). Similarly to that of complex **1** [21], the voltammogram shows a reversible redox wave for the ferrocene moiety at $E_{1/2}$ = 0.43 V/[FcH/FcH$^+$] followed by an irreversible process at 1.06 V/[FcH/FcH$^+$], that could be assigned to the oxidation of Rh(I). By analogy with **1**, we can assume that the oxidation process at 0.43 V is a one-electron oxidation of ferrocene to ferrocenium.

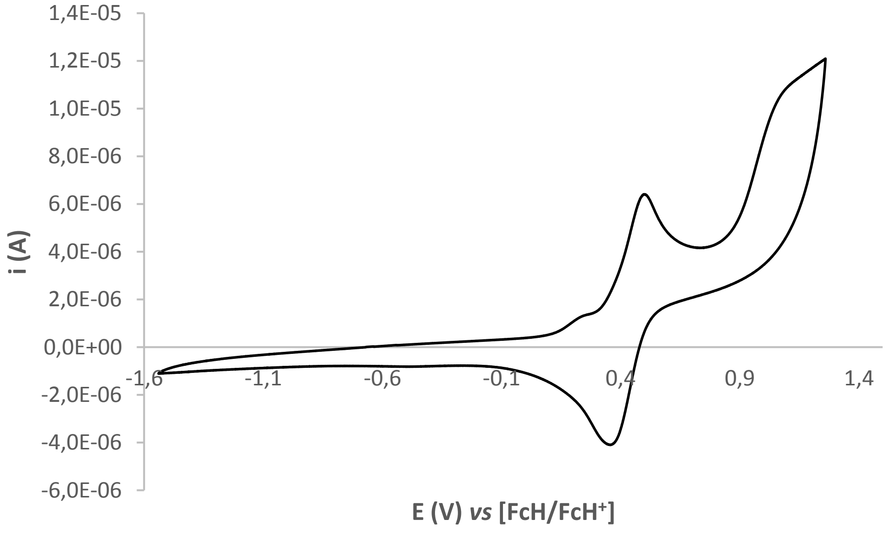

Figure 3. Cyclic voltammogram on a Pt electrode of complex **2**: 1 mM in CH_2Cl_2 with $n$$Bu_4NBF_4$ (0.1 M) at a scan rate of 0.2 V s^{-1}.

Although it was possible to generate the oxidised complexes by bulk electrolysis, we ruled this procedure out for preparative purposes since it could be difficult to separate the expected product from the ionic supporting electrolyte. We thus turned to chemical oxidation. The choice of oxidant was guided by the $E_{1/2}$ values of the ferrocene/ferrocenium redox couple, obtained via electrochemical methods, but other parameters had to also be taken into account, such as the "innocent" character of the reagent and the ease of purification of the oxidised Rh complex [30]. $NOBF_4$ is a strong oxidant but reacted with the phosphine group, giving a phosphine oxide. $AgBF_4$ was the most obvious choice, however its oxidation potential is very solvent-dependent and should perform the oxidation of the ferrocenyl moiety in **1** and **2** in CH_2Cl_2 (E°= 0.65 V/[FcH/FcH$^+$]), but not in a coordinating solvent like MeCN (E°= 0.04 V/[FcH/FcH$^+$]). We therefore focused our attention on thianthrenium tetrafluoroborate [Th][BF_4] (E°= 0.86 V/[FcH/FcH$^+$] in MeCN), the oxidation potential of which does not vary much with the solvent [22]. [Th][BF_4] gives deep purple solutions in acetonitrile and is insoluble in ether, whereas its reduced form is colourless and soluble in ether. This means that the reactions can be followed visually and that the oxidised rhodium complexes may be purified by simple precipitation and washing with Et_2O.

Chemical oxidation of complexes **1** and **2** in dichloromethane

Complex **1** was oxidised in CH_2Cl_2, either by addition of solid, anhydrous $AgBF_4$ [31], or by a [Th][BF_4] solution in the same solvent at room temperature (scheme 2). The orange dichloromethane solution turned rapidly olive-green, at which point it was concentrated to ca. 0.5 mL, and diethyl ether was added. A dark green precipitate separated from the light yellow solution, which was filtered off. The green solid was further rinsed with diethyl ether and analysed by ^{1}H and ^{31}P NMR in CD_2Cl_2 (fig. 4).

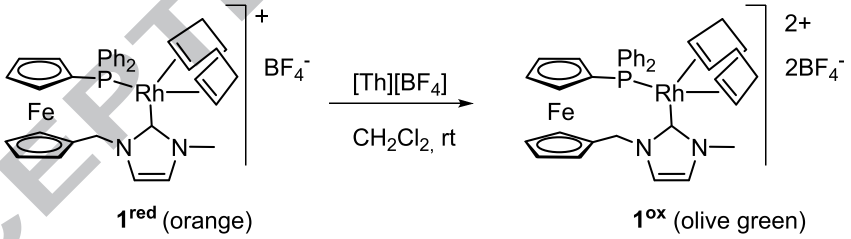

Scheme 2. Oxidation of rhodium(I) complex **1** with [Th][BF_4] in CH_2Cl_2.

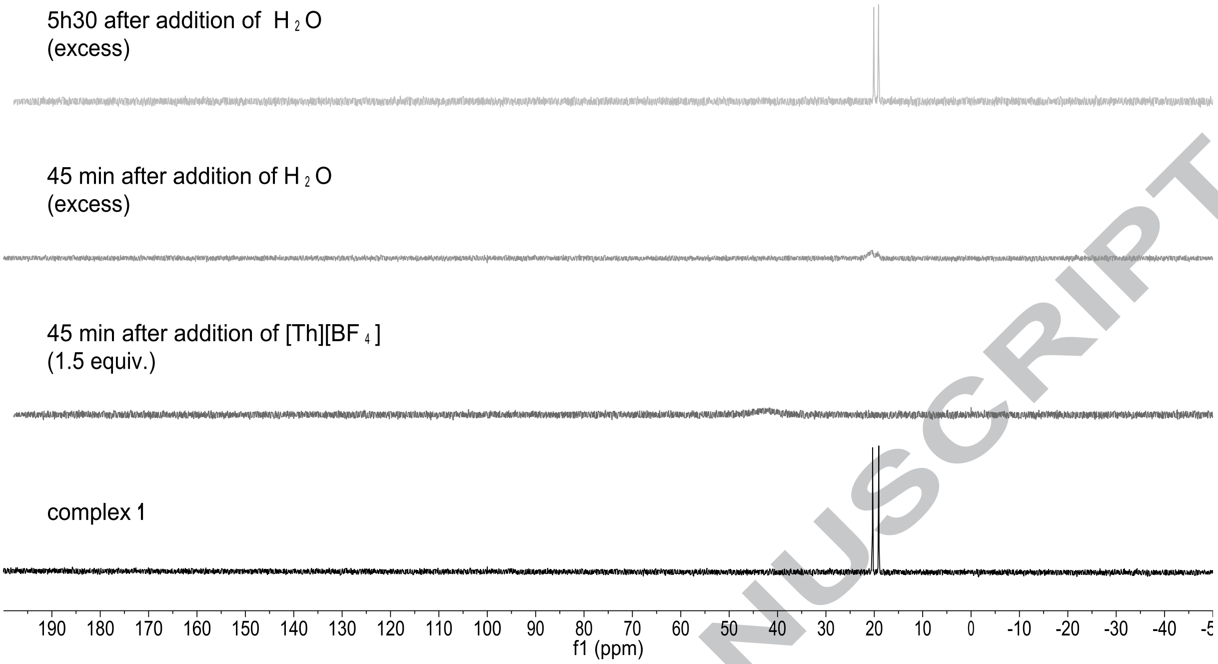

Figure 4. ^{31}P NMR spectra: oxidation of complex **1** by [Th][BF$_4$] in CD_2Cl_2.

The ^{1}H NMR spectrum showed very broad signals stretching from δ 25 to -10, whereas no or very weak shifted signals were detected by ^{31}P NMR. The characteristic colour and the absence of ^{31}P NMR signal suggested to us that we had generated paramagnetic ferrocenium. The reversible nature of this oxidation was demonstrated when excess water was added to the green CD_2Cl_2 solution [32]: the solution became orange again and its ^{31}P NMR spectrum showed a doublet at δ 19.5 with a coupling constant of 158 Hz. Purification of the NMR sample by simple drying and filtration on neutral alumina allowed the complete recovery of the starting Rh(I) complex.

It has been demonstrated by Wrighton *et al.* that infra-red ν_{CO} values in transition metal carbonyl complexes with ferrocenylphosphino ligands could be increased by up to 20 cm^{-1} upon oxidation of ferrocene [11]. More recently, Bielawski *et al.* measured the values for a carbonyl rhodium complex bearing a diaminocarbene-ferrocenophane ligand in both reduced and oxidised states, and found on average a difference of 20 cm^{-1} between the two oxidation states [33]. Infra-red thus appeared to us as a powerful tool to demonstrate the influence of ferrocene oxidation state on the electron density at rhodium in our complexes. In a typical procedure, solid, anhydrous $AgBF_4$ (1.5 equiv.) was used to generate the oxidised form of carbonyl complex **2** in CH_2Cl_2 (scheme 3). The colour turned in a few seconds from light yellow to forest green [34].

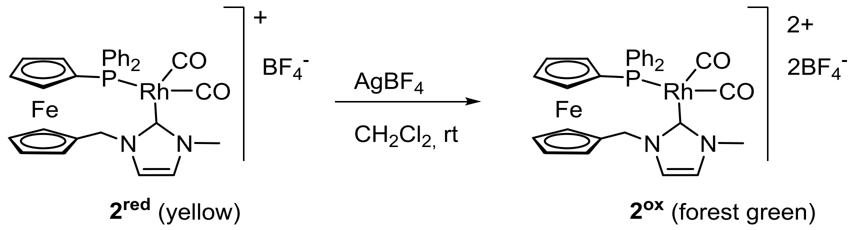

Scheme 3. Oxidation of rhodium(I) carbonyl complex **2** with $AgBF_4$ in CH_2Cl_2.

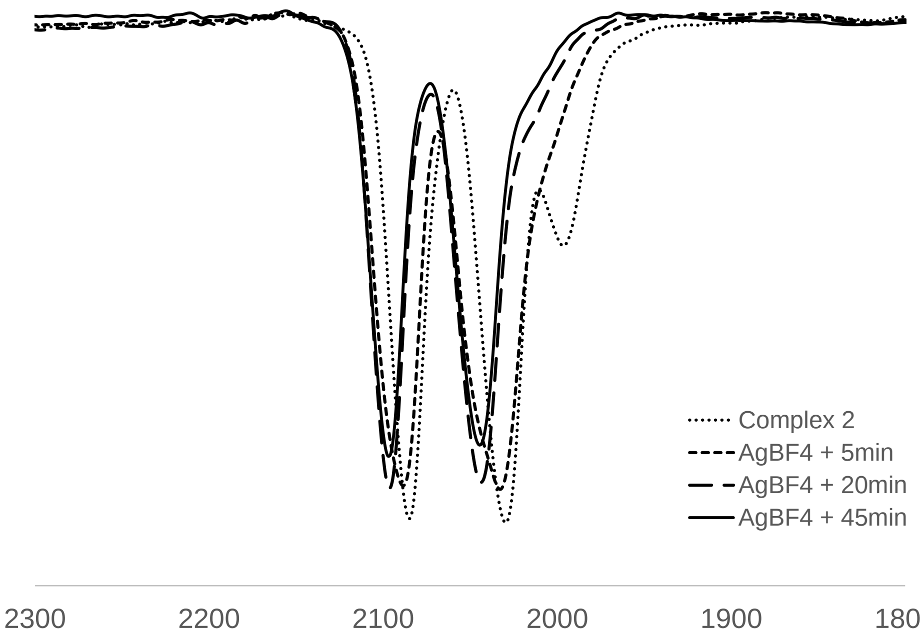

Figure 5. IR spectra (ATR), oxidation of complex **2** with $AgBF_4$ in CH_2Cl_2. $\nu_{CO}(\mathbf{2}^{\mathbf{red}})$, cm^{-1}: 2084, 2029; after 45min, $\nu_{CO}(\mathbf{2}^{\mathbf{ox}})$, cm^{-1}: 2097, 2045. The small band at 1997 cm^{-1} for the initial solution is attributed to a monocarbonyl impurity (see Experimental section).

IR spectra were taken at intervals and showed the shift of the original ν_{CO} bands to higher stretching frequencies by 13 cm^{-1} for the higher frequency band and by 16 cm^{-1} for that at lower frequency (fig. 5) [35]. This is characteristic of a metal centre with a lower electron density, since decreased backbonding from the d-orbital of the metal to the π^* antibonding orbital strengthens the CO bonds and shifts the ν_{CO} bands toward higher frequencies. The average difference between the ν_{CO} values for $\mathbf{2}^{\mathbf{red}}$ and $\mathbf{2}^{\mathbf{ox}}$ is 14 cm^{-1}, which is significant enough to assert that the reactivity at the rhodium centre may be affected by the oxidation of the ferrocene unit.

Chemical oxidation of complexes **1** and **2** in acetonitrile

As $AgBF_4$ has a redox potential of 0.04 V/[FcH/FcH$^+$] in MeCN [29], it should not be capable of oxidizing the ferrocene moiety of **2**. We therefore turned to [Th][BF$_4$], which possesses the additional advantage of being very soluble in this solvent. Typically, a solution of

[Th][BF$_4$] in MeCN was added dropwise to a solution of complex **2** in the same solvent (scheme 4). As reported earlier in the case of **1**, we observed a very different behaviour from the reaction in dichloromethane: no colour change to green was detected. Rather, a brown-orange solution was obtained after the addition of ca. 1.5 equivalent of oxidant. At the end of the addition, the solvent was evaporated to a minimum and diethyl ether was added to precipitate the rhodium complex and wash off the products of [Th][BF$_4$] reduction as well as unreacted **2**.

The ^{31}P NMR spectrum of the crude reaction mixture showed one major species appearing as a doublet at δ 41.5, with a coupling constant of 138 Hz, along with some unreacted **2**, whereas the ^{1}H NMR spectrum was typical of a diamagnetic compound, and revealed the presence of bound acetonitrile molecules. We demonstrated earlier, for the oxidation of **1** in acetonitrile, that the species showing a doublet at δ 41.5 is a rhodium(III) complex resulting from the oxidation of the ferrocene unit to ferrocenium and subsequent electron transfer from rhodium to ferrocenium [21]. The reorganisation of the coordination sphere around rhodium to adopt the preferred octahedral geometry implied coordination of acetonitrile molecules. An unusual C-H activation at ferrocene followed this reorganisation to give the air-stable rhodium(III) complex **3**. Here we demonstrate that the oxidations of complex **1** (bearing a COD ligand) and the dicarbonyl complex **2** lead to the same species (scheme 4). The full characterization of the product **3**, which includes the X-ray diffraction analysis of a bipy derivative, is reported in our previous contribution [21].

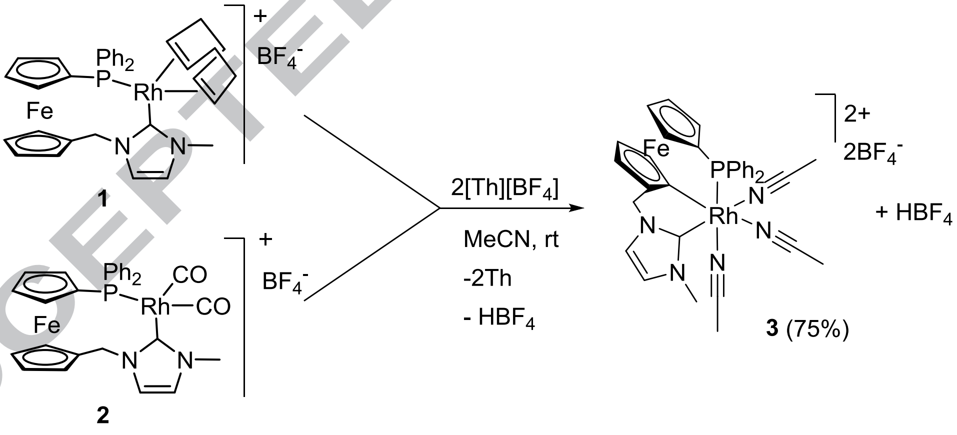

Scheme 4. Oxidation of complexes **1** and **2** with [Th][BF$_4$] in MeCN.

The reaction of the carbonyl complex **2** was also followed by ^{31}P NMR (fig. 6). The species giving a doublet at δ 28.7 was previously shown to be the intermediate rhodium(III) species (**4**) that has not yet undergone the C-H activation at ferrocene (scheme 5): it was the main species observed after 10 min, along with some unreacted **2** and an unidentified by-product at δ *ca*. 25. Oxidation of rhodium(I) to rhodium(III) is thus very quick and is followed by the slow C-H activation at ferrocene to give complex **3** as the main species after 24 h.

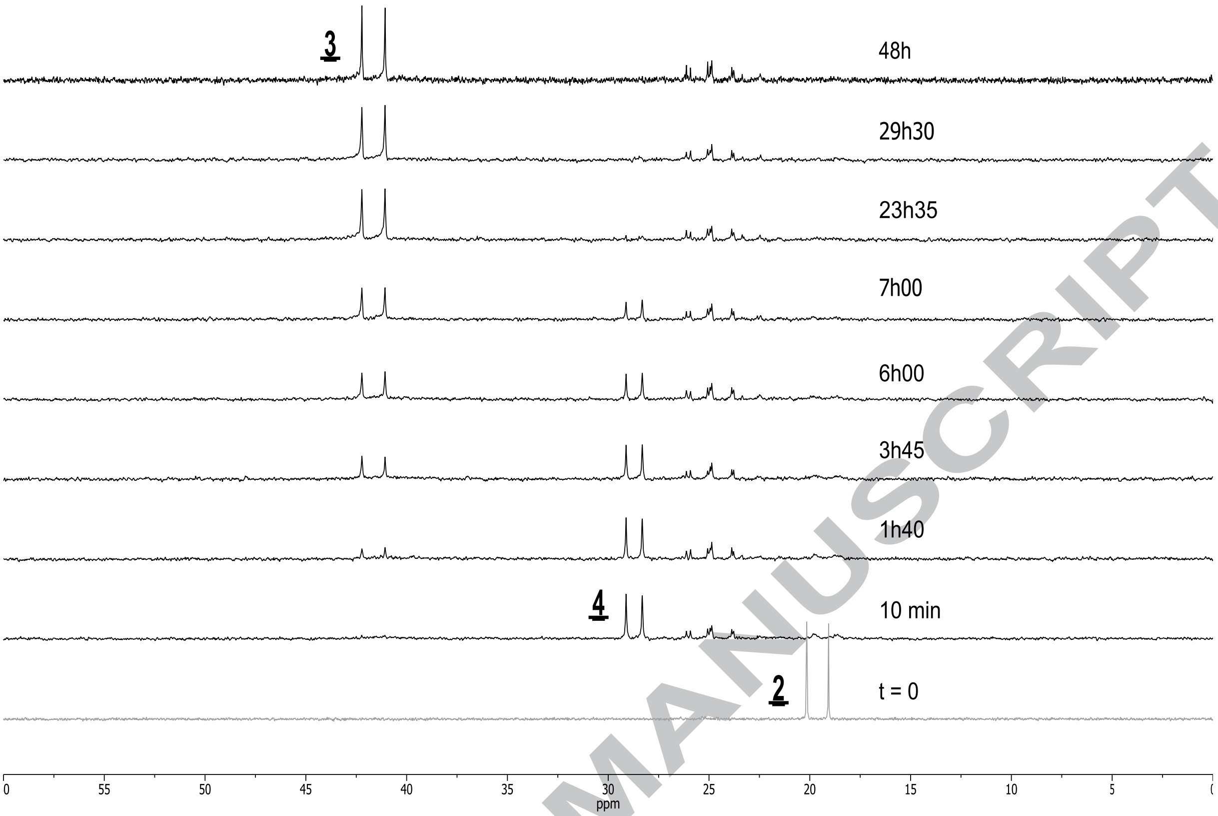

Figure 6. ^{31}P NMR spectra: oxidation of complex **2** by [Th][BF$_4$] in MeCN.

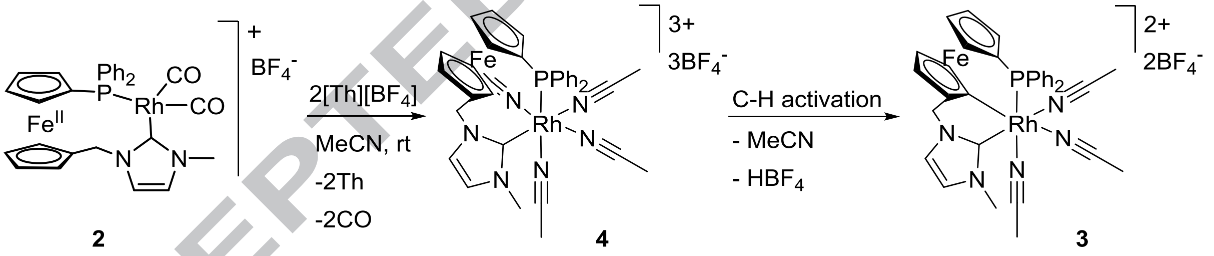

Scheme 5. Intermediate species (**4**) in the oxidation process of Rh^{I} complex **2** to Rh^{III} complex **3**.

In order to check that ferrocene could efficiently act as an electron relay, complex **2** was first oxidized in CH_2Cl_2 with an excess of $AgBF_4$ (1.5 equiv.), giving rise to the forest-green, paramagnetic ferrocenium-Rh(I) complex **2^{ox}** (scheme 6). After filtration of insoluble silver, the solution was evaporated *in vacuo* to give a green solid: upon addition of MeCN, the colour instantly turned to orange-brown. After 24h standing at room temperature, the solvent was evaporated and the orange residue analysed by ^{31}P and ^{1}H NMR. The ^{31}P NMR spectrum revealed the presence of two species in *ca.* 75:25 ratio: the doublet situated at δ 41.6 ($J_{Rh\text{-}P}$ = 138 Hz), characteristic of complex **3**, and a doublet at δ 33.2 ($J_{Rh\text{-} P}$= 120 Hz) that might arise from the reaction of **2^{red}** with acetonitrile. The ^{1}H NMR spectrum confirmed the presence of complex **3** as the main product. The product distribution is consistent with the oxidation stoichiometry (two oxidizing equivalents are necessary to convert **2^{red}** to **3**).

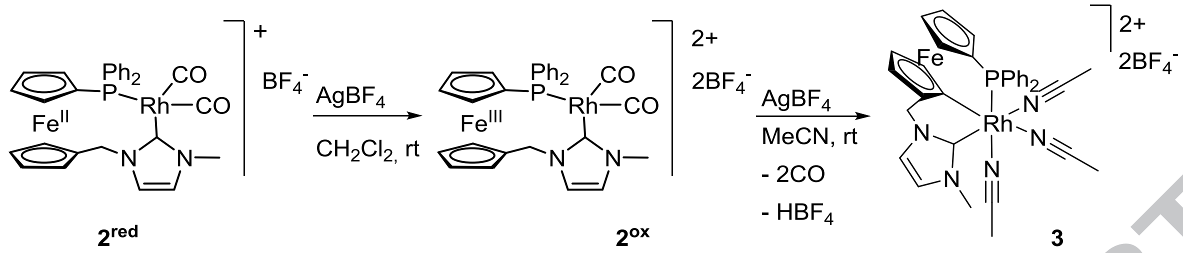

Scheme 6. Stepwise oxidation of complex **2** in CH_2Cl_2 and reaction of $\mathbf{2}^{ox}$ in MeCN.

The above combined results confirm that the reactivity of the rhodium centre can be enhanced dramatically, simply by changing the oxidation state of a ligand electronically connected to Rh. Thanks to this stepwise process and to the irreversible character of the reaction, it even becomes possible to use $AgBF_4$, a very common and convenient oxidant which is too weak to operate in acetonitrile.

3. Hydrosilylation catalysis

Rhodium(III) complexes, particularly half-sandwich Rh^{III} complexes, are catalysts of choice for the functionalization of C_{sp2}-H bonds [36-38] and we recently showed the potential of complex **3** for this type of reaction [21]. We envisioned that this system may also be suitable for other types of catalytic reactions, such as the hydrosilylation of carbonyl compounds. We previously described the use of complex **1** and its analogue bearing a norbornadiene ligand in place of COD as catalysts for this reaction but both proved rather sluggish, probably due to their high stability and the difficulty to remove the diene ligand [17].

Thus hydrosilylation of acetophenone and its derivatives were carried out with 1 mol% of complex **1** or **3** in THF at room temperature (scheme 7, table 2). All reactions were stopped after 17 h to allow for direct comparison of conversions.

Scheme 7, Table 2. Hydrosilylation of acetophenone derivatives.

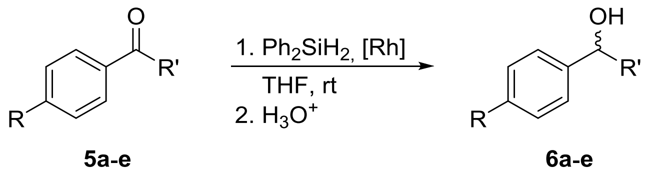

Entry	Substrate (R, R')	Product	Conversion (%) (b)	
			Complex **1**	Complex **3**
1	**5a** (H, Me)	**6a**	54 (1)	85 (4)
2	**5b** (Me, Me)	**6b**	43 (4)	88 (3)
3	**5c** (OMe, Me)	**6c**	53 (3)	90 (1)
4	**5d** (F, Me)	**6d**	50 (0)	78 (4)
5	**5e** (H, CF_3)	**6e**	>99	>99

(a) Reagents and conditions: acetophenone (1.0 equiv., 2M in THF), diphenylsilane (1.1 equiv.), Rh cat. (1mol%), rt, 17 h. (b) Average of two runs, with % difference between the two runs in parentheses; conversion calculated by integration of characteristic ^{1}H NMR signals of acetophenone derivative and 1-phenylethanol derivative in the crude reaction mixture after hydrolysis of the silyl ether.

As a general observation, the rhodium(III) complex **3** shows good activity for the hydrosilylation of both electron-rich and electron-deficient acetophenones and is a better catalyst than the rhodium(I) complex **1**. The reaction of diphenylsilane with acetophenone was followed by ^{1}H NMR in d_8-THF. The conversion of acetophenone into the expected silyl ether was plotted against time and the reaction profiles turned out surprisingly different for **1** and **3** (fig. 7) [39]. Comparison of the initial rates shows that the catalytic activity of **3** is 20 times greater than that of **1**. For complex **1**, the reaction follows a first order rate law, whereas the data for **3** do not appear consistent with a simple rate law.

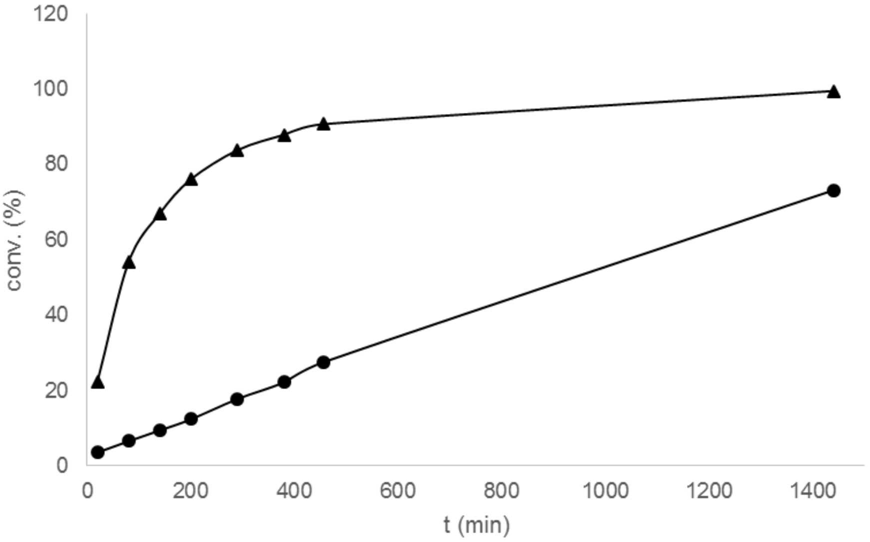

Figure 7. Reaction of Ph_2SiH_2 with acetophenone (1 mol% catalyst, d_8-THF, rt). Conversion (%) of acetophenone *vs.* time, circles: complex **1**; triangles: complex **3**.

Conclusions

A new dicarbonyl rhodium(I) complex bearing an electroactive ferrocenyl phosphine-NHC ligand has been synthesized and fully characterized. Its behaviour in the presence of a chemical oxidant has been studied, proving that the electron density at the rhodium centre could be tuned by oxidation of the ferrocenyl group on the bidentate ligand. This difference has been highlighted by infra-red spectroscopic measurement of the CO stretching frequencies. The dicarbonyl rhodium(I) complex has also shown an interesting reactivity in acetonitrile which parallels that of the related COD complex **1**, giving a stable rhodium(III) complex after several oxidation-electron transfer processes and complete reorganisation of the coordination sphere.

Acknowledgements

This work was supported by the Agence Nationale de la Recherche (ANR-07-JCJC-0041). We are also grateful to the CNRS (Centre National de la Recherche Scientifique) for further financial support.

Appendix A. Supplementary Data

CCDC 986640 contains the supplementary crystallographic data for compound **2**. This data can be obtained free of charge via http://www.ccdc.cam.ac.uk/conts/retrieving.html, or from the Cambridge Crystallographic Data Centre, 12 Union Road, Cambridge CB2 1EZ, UK; fax: +44 1223-336-033; or e-mail: deposit@ccdc.cam.ac.uk. Supplementary data associated with this article: crystal data and refinement parameters for compound **2**.

References

1. I.M. Lorkovic, M.S. Wrighton, W.M. Davis, J. Am. Chem. Soc., 116 (1994) 6220–6228.
2. C.S. Slone, C.A. Mirkin, G.P.A. Yap, I.A. Guzei, A.L. Rheingold, J. Am. Chem. Soc., 119 (1997) 10743–10753.
3. C.K.A. Gregson, V.C. Gibson, N.J. Long, E.L. Marshall, P.J. Oxford, A.J.P. White, J. Am. Chem. Soc., 128 (2006) 7410–7411.
4. K. Arumugam, C.D. Varnado, S. Sproules, V.M. Lynch, C.W. Bielawski, Chem.-Eur. J., 19 (2013) 10866–10875.
5. C.D. Varnado, Jr, E.L. Rosen, M.S. Collins, V.M. Lynch, C.W. Bielawski, Dalton Trans., 42 (2013) 13251–13264.
6. A.G. Tennyson, V.M. Lynch, C.W. Bielawski, J. Am. Chem. Soc., 132 (2010) 9420–9429.
7. E.M. Broderick, N. Guo, T. Wu, C.S. Vogel, C. Xu, J. Sutter, J.T. Miller, K. Meyer, T. Cantat, P.L. Diaconescu, Chem. Commun., 47 (2011) 9897–9899.
8. E.M. Broderick, N. Guo, C.S. Vogel, C. Xu, J. Sutter, J.T. Miller, K. Meyer, P. Mehrkhodavandi, P.L. Diaconescu, J. Am. Chem. Soc., 133 (2011) 9278–9281.
9. M. Süßner, H. Plenio, Angewandte Chemie International Edition, 44 (2005) 6885–6888.
10. R. Savka, S. Foro, M. Gallei, M. Rehahn, H. Plenio, Chem.- Eur. J., 19 (2013) 10655–10662.
11. T.M. Miller, K.J. Ahmed, M.S. Wrighton, Inorg. Chem., 28 (1989) 2347–2355.
12. A.M. Allgeier, C.S. Slone, C.A. Mirkin, L.M. Liable-Sands, G.P.A. Yap, A.L. Rheingold, J. Am. Chem. Soc., 119 (1997) 550–559.
13. I.V. Kourkine, C.S. Slone, C.A. Mirkin, L.M. Liable-Sands, A.L. Rheingold, Inorg. Chem., 38 (1999) 2758–2759.
14. I.M. Lorkovic, R.R. Duff Jr., M.S. Wrighton, J. Am. Chem. Soc., 117 (1995) 3617–3618.
15. D.A. Weinberger, T.B. Higgins, C.A. Mirkin, L.M. Liable-Sands, A.L. Rheingold, Angew. Chem. Int. Ed., 38 (1999) 2565–2568.
16. K.J. Blackmore, J.W. Ziller, A.F. Heyduk, Inorg. Chem., 44 (2005) 5559–5561.
17. A. Labande, J.-C. Daran, E. Manoury, R. Poli, Eur. J. Inorg. Chem., (2007) 1205–1209.
18. J. Wolf, A. Labande, J.-C. Daran, R. Poli, Eur. J. Inorg. Chem., (2007) 5069–5079.
19. N. Debono, A. Labande, E. Manoury, J.-C. Daran, R. Poli, Organometallics, 29 (2010) 1879–1882.
20. A. Labande, J.-C. Daran, N.J. Long, A.J.P. White, R. Poli, New J. Chem., 35 (2011) 2162–2168.
21. A. Labande, N. Debono, A. Sournia-Saquet, J.-C. Daran, R. Poli, Dalton Trans., 42 (2013) 6531–6537.
22. B. Boduszek, H. J. Shine, J. Org. Chem., 53 (1988), 5142-5143.
23. A. Altomare, M. Burla, M. Camalli, G. Cascarano, C. Giacovazzo, A. Guagliardi, A. Moliterni, G. Polidori, R. Spagna, J. Appl. Cryst., 32 (1999) 115-119.
24. G. M. Sheldrick, Acta Cryst. A, 64 (2008) 112-122.
25. L. J. Farrugia, J. Appl. Cryst., 30 (1997) 565.
26. L.D. Field, B.A. Messerle, K.Q. Vuong, P. Turner, Organometallics, 24 (2005) 4241–4250.
27. L.D. Field, B.A. Messerle, K.Q. Vuong, P. Turner, Dalton Trans., (2009) 3599–3614.
28. S. Burling, L.D. Field, H.L. Li, B.A. Messerle, P. Turner, Eur. J. Inorg. Chem., 2003 (2003) 3179–3184.
29. C.H. Leung, C.D. Incarvito, R.H. Crabtree, Organometallics, 25 (2006) 6099–6107.
30. N.G. Connelly, W.E. Geiger, Chem. Rev., 96 (1996) 877–910.

31. The quality of $AgBF_4$ is crucial since only traces of water lead to the reduction of ferrocenium.
32. H_2O reduces ferrocenium back to ferrocene in complex **1** but the nature of the oxidized species was not investigated yet.
33. D.M. Khramov, E.L. Rosen, V.M. Lynch, C.W. Bielawski, Angew. Chem. Int. Ed., 47 (2008) 2267–2270.
34. $\mathbf{2}^{\mathbf{ox}}$ is very sensitive to moisture and turned rapidly from forest green to brown when exposed to traces of water to give a complex mixture.
35. The third band of medium intensity at 1997 cm^{-1} may be attributed to the monocarbonyl complex due to an incomplete reaction (^{31}P NMR: >95% of dicarbonyl complex in this sample).
36. D.A. Colby, R.G. Bergman, J.A. Ellman, Chem. Rev., 110 (2010) 624–655.
37. J. Wencel-Delord, T. Droge, F. Liu, F. Glorius, Chem. Soc. Rev., 40 (2011) 4740–4761.
38. G. Song, F. Wang, X. Li, Chem. Soc. Rev., 41 (2012) 3651–3678.
39. The amount of silyl enol ether by-product was neglected in the calculations since it represents less than 1% of the total.

The behaviour of a new dicarbonyl rhodium(I) complex bearing an electroactive ferrocenyl phosphine-NHC ligand towards oxidation has been studied, proving that the electron density at the rhodium centre could be tuned by oxidation of the ferrocenyl group. This difference has been highlighted by infra-red spectroscopic measurements.

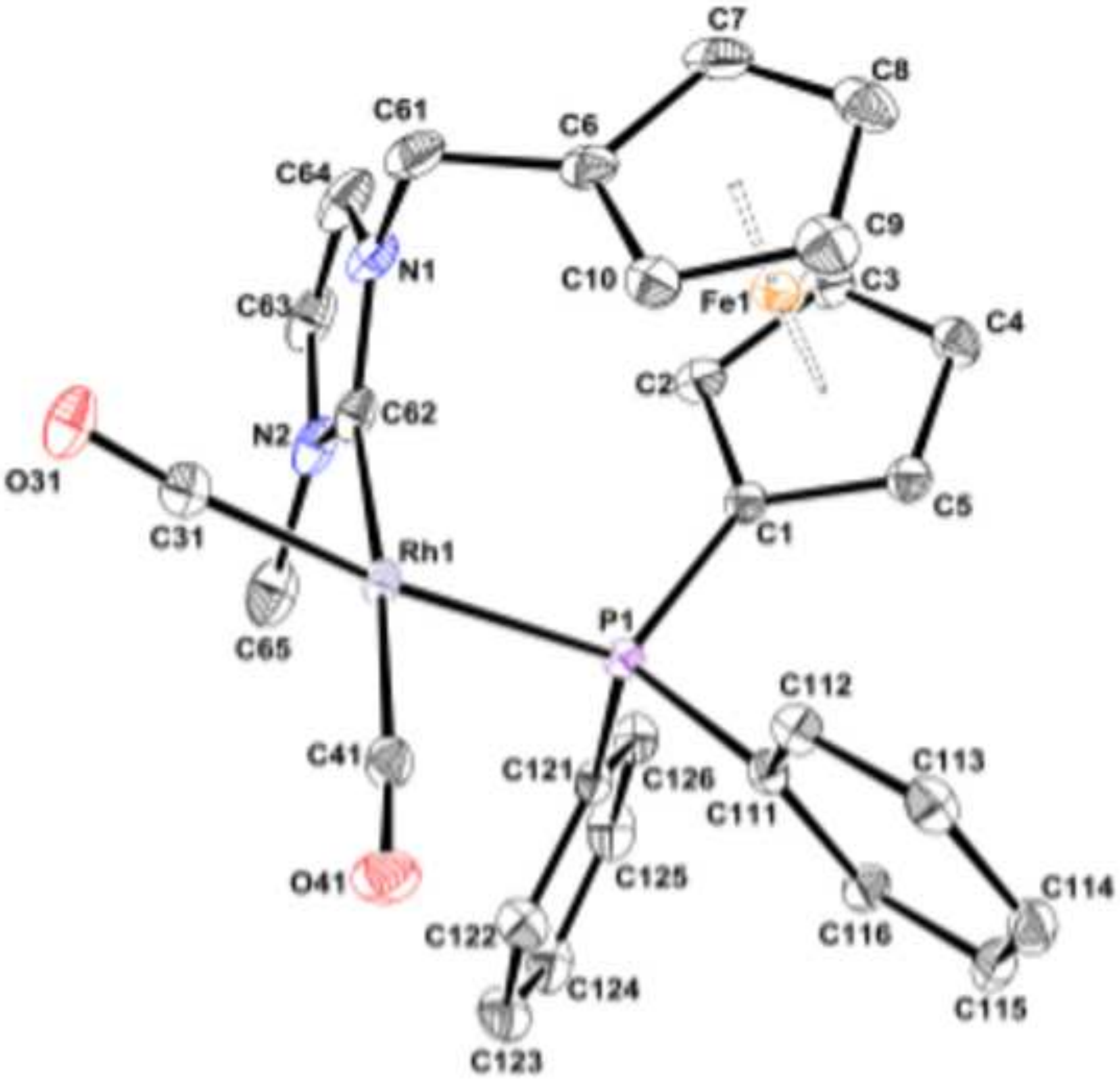
C7
C8
C61
C6
C64
C9
N1
C10
C3
Fe1
C4
C63
C2
C62
N2
O31
C31
C5
C1
Rh1
C65
P1
C112
C41
C113
C121
C126
C111
O41
C125
C114
C122
C116
C124
C115
C123